Rotary Triboelectric Nanogenerator Based on a Hybridized Mechanism for Harvesting Wind Energy

Yannan Xie,[†,‡,⊥] Sihong Wang,[†,⊥] Long Lin,[†] Qingshen Jing,[†] Zong-Hong Lin,[†] Simiao Niu,[†] Zhengyun Wu,[‡] and Zhong Lin Wang[†,§,*]

[†]School of Materials Science and Engineering, Georgia Institute of Technology, Atlanta, Georgia 30332-0245, United States, [‡]Department of Physics, Xiamen University, Xiamen 361005, Fujian, China, and [§]Beijing Institute of Nanoenergy and Nanosystems, Chinese Academy of Sciences, Beijing, China. [⊥]These authors contributed equally.

ABSTRACT Harvesting mechanical energy is becoming increasingly important for its availability and abundance in our living environment. Triboelectric nanogenerator (TENG) is a simple, cost-effective, and highly efficient approach for generating electricity from mechanical energies in a wide range of forms. Here, we developed a TENG designed for harvesting tiny-scale wind energy available in our normal living environment using conventional materials. The energy harvester is based on a rotary driven mechanical deformation of multiple plate-based TENGs. The operation mechanism is a hybridization of the contact-sliding-separation-contact processes by using the triboelectrification and electrostatic induction effects. With the introduction of polymer nanowires on surfaces, the rotary TENG delivers an open-circuit voltage of 250 V and a short-circuit current of 0.25 mA, corresponding to a maximum power density of ~39 W/m^2 at a wind speed of ~15 m/s, which is capable of directly driving hundreds of electronic devices such as commercial light-emitting diodes (LEDs), or rapidly charging capacitors. The rotary TENG was also applied as a self-powered sensor for measuring wind speed. This work represents a significant progress in the practical application of the TENG and its great potential in the future wind power technology. This technology can also be extended for harvesting energy from ocean current, making nanotechnology reaching our daily life a possibility in the near future.

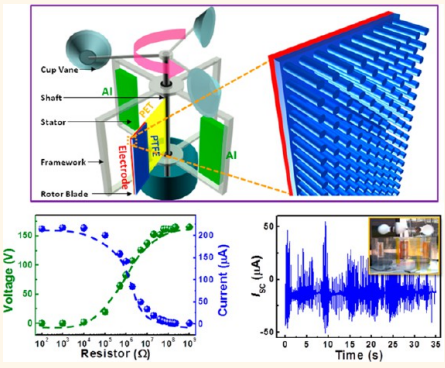

KEYWORDS: mechanical energy harvesting · triboelectric nanogenerators · wind power · self-powered sensors

Because of the rapid development of miniaturized and portable electronics, new technologies that can harvest energy from our daily living environment as sustainable and self−sufficient micro/nanopower sources are highly desirable.[1,2] Recently, nanogenerators (NGs)[3−7] have been actively developed since 2006 for converting small-scale mechanical energy into electricity. Wind energy, as a key mechanical energy offered by nature, has been regarded as one of the most important renewable and green energy sources under the threat of the global warming and energy crisis.[8,9] The conventional approach of generating electricity from wind relies on the structure of wind turbines and the principle of electromagnetic induction.[10] However, there are several drawbacks of this kind of device, including large size and weight, high cost of installation, difficulty of being driven under low wind speeds, and thus low efficiency, which limits its usability especially for the weak wind in our daily living environment such as around houses and in the city.[11] Recently, piezoelectric windmills employing piezoelectric bimorph transducer structures have been reported with low start-up speed and small sizes.[12−14] However, the structures are still complex and the outputs are relatively low. In this regard, developing innovative concepts and strategies is of great necessity for extending the applications of low-magnitude wind in our living environment.

Recently, triboelectric nanogenerators (TENGs),[15,16] with the advantages of simple fabrication, excellent reliability, large output power, high efficiency, and low cost, have been invented based on the triboelectric effect,[17−20] which is a universally known,

* Address correspondence to zlwang@gatech.edu.

Received for review May 15, 2013 and accepted June 12, 2013.

Published online June 14, 2013
10.1021/nn402477h

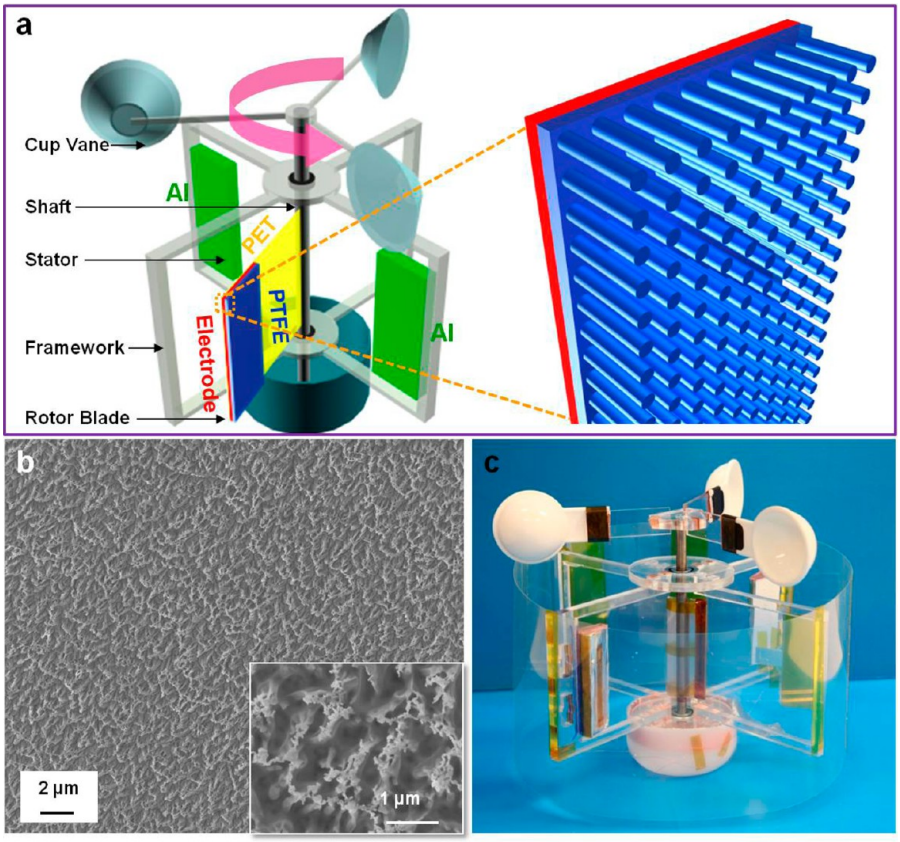

Figure 1. Device structure of the rotary triboelectric nanogenerator (R-TENG). (a) The schematic diagram showing the structural design of the R-TENG, with the enlarged picture showing the nanowire-like structures on the surface of PTFE. (b) The SEM image of the PTFE surface with etched nanowire-like structures; the inset is an SEM image of the nanowires. (c) A photograph of the fabricated R-TENG.

but generally regarded as an undesirable phenomena in electronic systems. The TENGs generate electricity from mechanical motions through the coupling of triboelectrification and electrostatic induction: the periodic contact and separation between two different surfaces with oppositely polarized triboelectric charges can cyclically change the induced potential difference across two electrodes, thus driving the alternating flow of electrons through an external load.[21−23] In practical applications, such an electricity generation process can be realized by any mechanical motions that can induce this periodic contact and separation of two surfaces either in a vertical direction contact-separation mode[21−23] or in-plane cycled sliding mode.[24−26]

In this paper, we developed a rotary structured triboelectric nanogenerator (R-TENG) for scavenging weak wind energy in our environment. Under the wind flow, the wind-cup structure will be driven to rotate and thus the soft and flexible polytetrafluoroethylene (PTFE) film based rotor blade will sweep across the Al sheets based stators consecutively, so that a repeating process of contact-sliding-separation-contact between the two charged surfaces can be achieved by hybridizing the two modes. On the basis of this new design, an open-circuit voltage (V_{OC}) of 250 V and short-circuit current (I_{SC}) of 0.25 mA have been reached, corresponding to a maximum power output of 62.5 mW, which is capable of either driving hundreds of electronic devices (such as commercial LEDs) instantaneously or efficiently charging energy storage units. Furthermore, we also demonstrated its potential application as a self-powered active wind speed sensor based on the distinct relationships between the electrical outputs and the wind speed. For the first time, a combination of TENG with traditional wind power technology is demonstrated for efficiently converting wind energy into electricity, which is an important progress in the practical applications of nanogenerators and also exhibits enormous potential as the future wind power technology.

RESULTS AND DISCUSSION

The structure of the R-TENG springs from the conventional wind cup structure, which includes a framework, a shaft, a flexible rotor blade, two stators, as illustrated in Figure 1a. The framework for supporting the entire structure consists of two Acrylic rectangles that are joined together perpendicularly at the common central axes, where the metallic shaft rod is positioned through two bearings. A flexible and soft rotor blade structurally made of a polyester (PET) film (~125 μm in thickness) is connected to the shaft, and

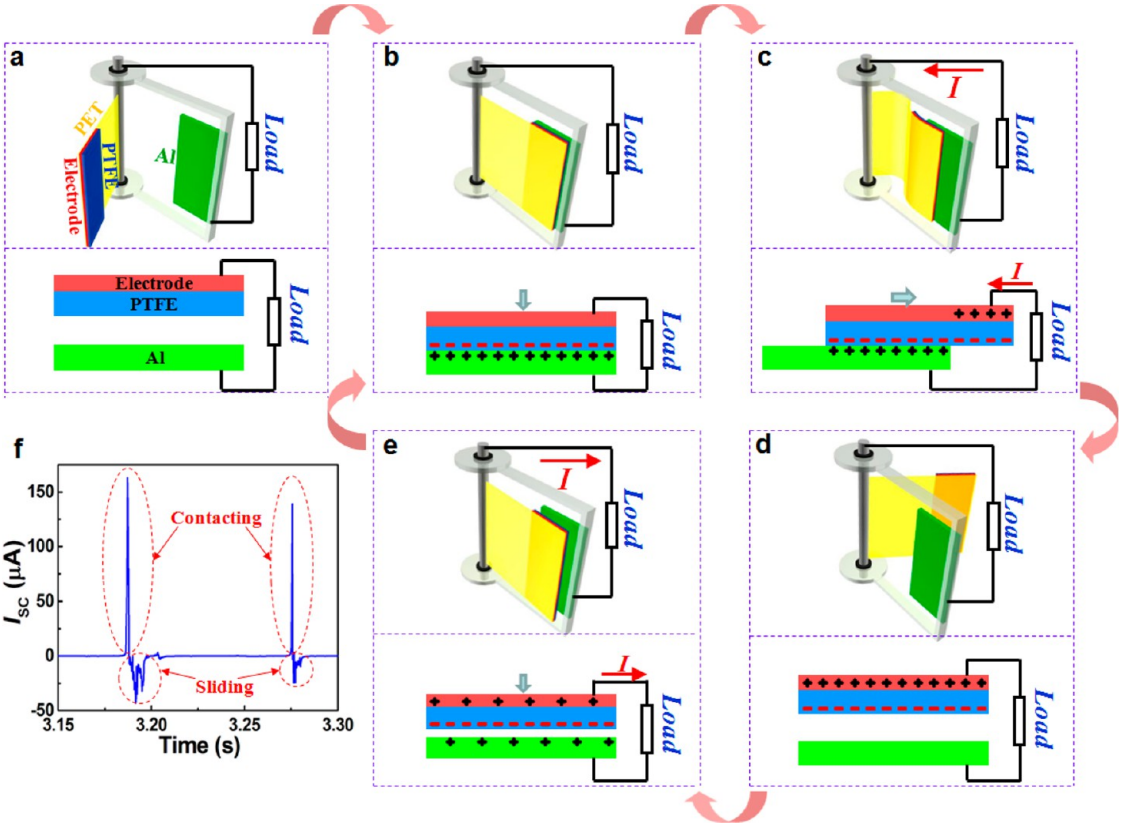

Figure 2. Working mechanism of the R-TENG based on a hybridization of contact-sliding-separation-contact processes. Three-dimensional (upper) and cross-sectional (bottom) sketches of: (a) original position without wind blow; (b) PTFE is brought into contact with Al stator; (c) PTFE is sliding apart from the Al surface; (d) PTFE is separated from Al stator; and (e) PTFE approaching to the next Al stator. (f) The typical profile of the current output from the R-TENG.

thus can rotate with the shaft. Around the circumference of the device, two Al covered plates as the symmetric stators stretch out from the framework toward the shaft direction. On top of the shaft, the wind cup setup is mounted to convert the wind flow into the rotation of the shaft and the flexible rotor, during which the rotor blade will periodically sweep across the stators with small resistance. In this process, a consecutive face-to-face contact (in area of 2.5 cm × 6.4 cm) and separation between the rotor and the stators will be enabled, which can serve as the basic TENG-based process for generating electricity. According to the triboelectric series,[27] a PTFE film was chosen to adhere at the end of the PET blade as a triboelectric layer to get into contact with Al that acts not only as the counter triboelectric layer, but also as an electrode. For the other electrode, a layer of metal film was deposited between the PTFE and PET to enable the transfer of induced charges. To enhance the surface roughness and therefore improve the triboelectric charge density,[16,21] the PTFE film was dry-etched through inductively coupled plasma (ICP) reactive ion etching to prepare nanowire-like structures on the surface[28] (with the magnified scheme in Figure 1a). As shown in the scanning electron microscopy (SEM) images, after a 40-s etching, the nanowire-like structures were uniformly distributed on the surface of PTFE, with an average length of ~700 nm (Figure 1b). The photograph of an as-fabricated R-TENG device is shown in Figure 1c. We can find that this device is light in weight, compact in size, cheap in cost, and robust in operation.

The electricity generation of the R-TENG is a hybridization of contact-sliding-separation-contact processes, as schematically depicted in Figure 2. In the original state where the rotor blade is stationary and the triboelectric layers are separated from each other (Figure 2a), there is no tribo-charges generated on the surfaces. When the wind blows on the wind cups, the rotor blade will be driven to rotate around the shaft, which will bring the PTFE film into full contact with the Al on either one of the stators (Figure 2b). Owing to the different tendencies to gain or lose electrons, the triboelectric effect will enable the generation of surface charges at the contact area due to relative sliding, leaving the PTFE with net negative charges and the Al with positive charges. At this very moment, because the opposite charges on the contact surfaces are in equal densities and locate at the same plane,[24,25,29,30] there is little electric potential difference generated in the space. As the polymeric rotor blade continues to rotate, the flexible blade will be bent in order to sweep across the rigid stator (Figure 2c). Because of the strong electrostatic

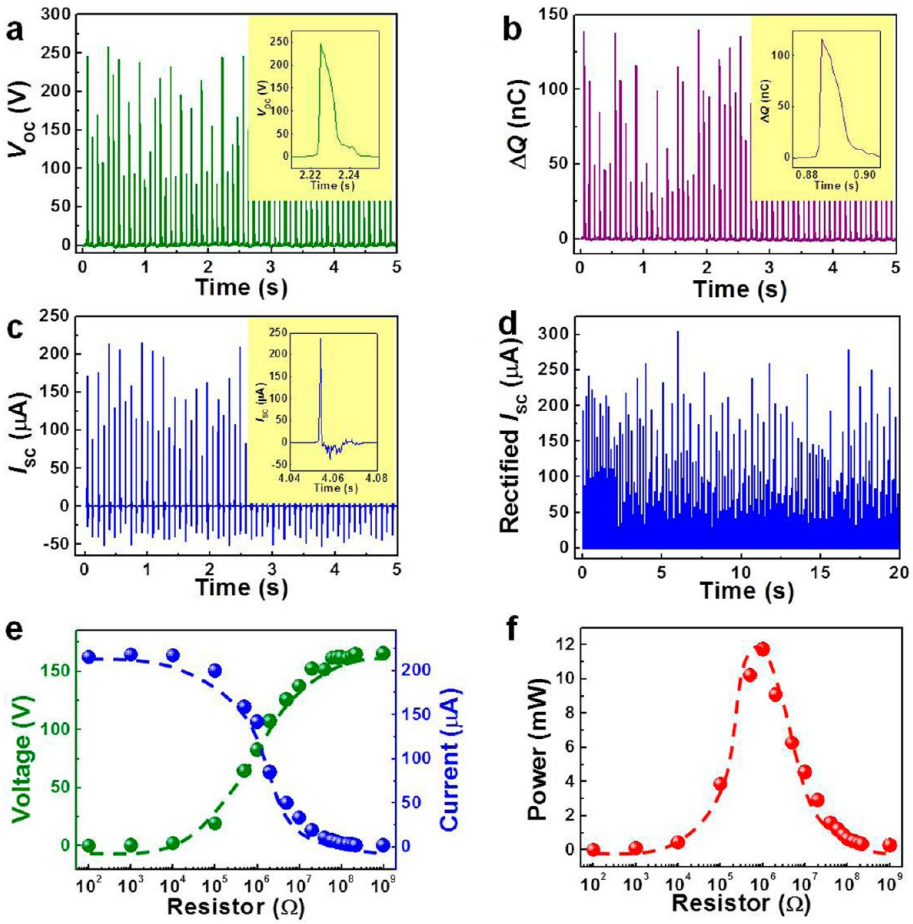

Figure 3. Performance of the R-TENG driven by the wind flow. (a) The open-circuit voltage (V_{OC}), (b) the transferred charges (ΔQ), (c) the I_{SC}, and (d) the rectified I_{SC} under the wind speed of 15 m/s (in the scale of 7 BF). (e and f) The dependence of (e) the output voltage (green) and current (blue) and (f) the power (red) on the resistance of the external load.

attraction between the two tribo-charged surfaces, the PTFE film has the tendency to keep the intimate contact with the Al stator, so that most of the bending happens on the PET portion of the rotor blade. The PTFE plate will be guided to slide outward across the Al surface, leading to a continuous decrease in the overlapping area of the two tribo-charged surfaces and thus the in-plane charge separation. The lateral dipole moment in parallel to the sliding surface will generate a higher potential on the Al surface, thus drives a current flow in the external load from the Al to the electrode of PTFE to offset the tribo-charge-induced potential. This process will last until the PTFE fully slides out of the Al surface, and the total transferred charges will equal the amount of the triboelectric charges on each surface. This is the working mechanism of the TENG in the sliding mode, which can help to generate higher triboelectric charge densities because the sliding provides much more friction than the contact mode, and it is more effective for triboelectrification.[24] Subsequently, the rotor blade will continue to rotate toward the other stator, with the attached electrode having positive charges with equal density of the negative tribocharges on the PTFE surfaces (Figure 2d).[31] When the rotor blade approaches the other Al blade, the two surfaces will get into contact momentarily in vertical direction (Figure 2e). An electric potential difference pointing from the electrode on the PTFE to the Al sheet will be generated, driving a reversal current flow in order to reach the electrostatic equilibrium where all of the positive charges on the PTFE electrode have transferred back to the Al stator. This is the working mechanism of the TENG in the contact-separation mode. At this point, a cycle is completed. Thus, the entire electricity generation process of the R-TENG hybridizes the in-plane contact-sliding mode and the separation-contact mode in vertical direction as a full cycle process and generates a pair of alternating currents: one lower-magnitude but wider peak corresponding to the in-plane charge separation and one sharper but narrower peak corresponding to the vertical charge recontact (Figure 2f).

The electrical output measurement of the R-TENG was carried out under a wind speed of ~15 m/s. In the process of separation-contacting-sliding-separation, the open-circuit voltage (V_{OC}) jumped from zero to a peak value of ~250 V and to zero again (Figure 3a), with the positive probe connecting to the electrode of the

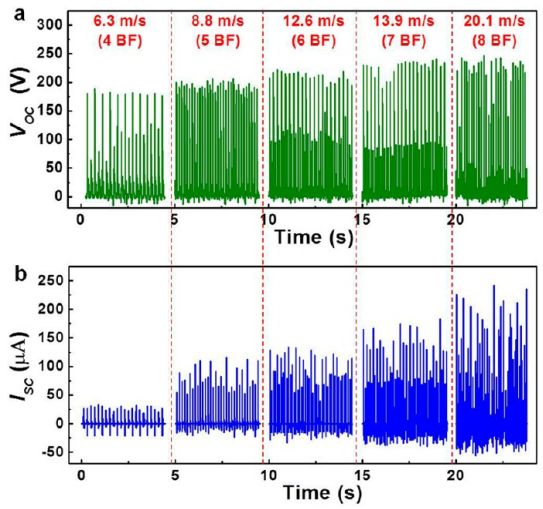

Figure 4. Influence of the wind speed on the electrical outputs. (a) The V_{OC} and (b) the I_{SC} under different wind speeds from 6.3 m/s (4 BF) to 20.1 m/s (8 BF).

PTFE film. The transferred charges (ΔQ) driven by this potential difference were also measured, as illustrated in Figure 3b, and the charges with a maximum amount of 140 nC flew back and forth between the two electrodes when the two tribo-charged surfaces were contacted and separated with each other. Consequently, the transfer of the charges produced an alternating-current (AC) output with a peak short-circuit current (I_{SC}) of 250 μA corresponding to the vertical contact process (Figure 3c). The amount of the transferred charges can also be obtained through the integration of each current peak over time (Figure S1). The total charges ΔQ generated from the sharp peak corresponding to the vertical-contact process equal those from the wider peak from sliding-separation process (Figure S1). From the enlarged profiles of the V_{OC}, ΔQ and I_{SC} shown in the insets of Figure 3a–c, the differences in the characteristics of the contacting mode and the sliding mode are clearly reflected: the steep increases of the V_{OC} and ΔQ with a sharp and higher I_{SC} peak for the vertical contact; the gradual decreases of the V_{OC} and ΔQ with a wider and lower I_{SC} peak for the sliding separation. This AC output can be rectified to a DC output by a full-way rectifying bridge, as shown in Figure 3d. After the rectification, the current output retained the same magnitude. Besides the V_{OC} and I_{SC}, the relationship between the effective output power and the resistance of external load is another important characteristic of the R-TENG. We have experimentally studied the voltage and current outputs on a series of different resistors. As depicted in Figure 3e, the current drops with the increase of the external resistance, while the voltage across the load follows a reversed tendency. Consequently, the instantaneous power on the load reaches a maximum value of ~12 mW when driving the load with a resistance of ~1 MΩ (Figure 3f).

To find the optimized number of stators in the R-TENG structure for the most effective electricity generation, we also fabricated similar R-TENG devices with 3 stators and 4 stators, respectively, as comparisons. As shown in Figure S2, driven by a wind with the same speed of 13 m/s, the R-TENG with 2 stators generates the largest and most stable electrical output. The probable reason is that with the increased stators, there will be less space in between for the rotors to recover to their original shape from the bending state after sweeping across the last stator, thus deteriorating the effective contact between the PTFE surface and the Al stator. Therefore, the R-TENG with 2 stators as we proposed is the best structure for the effective wind energy harvesting in the current design.

To investigate the relationships between the electric outputs of the R-TENG and wind speed, a systematic measurement was performed under different wind speeds from 6.3 m/s (4 BF in Beaufort wind force scale) to 20.1 m/s (8 BF). As shown in Figure 4a, with the wind speeds being raised, the V_{OC} first shows a small increase trend at lower wind speeds and then reaches a saturated value of 250 V. This result can be explained by the change in the surface charge density. The higher the wind speed, the larger rotational torque obtained by the polymer films, which means a larger contacting force. Since the PTFE surface was patterned with nanowire-like structures, a larger force applied will make the two surfaces contact more intimately, resulting in a higher surface charge density. But this will reach a saturated value after the contacting force is large enough.[16,21,23] As for the I_{SC}, the peak heights present a very obvious increasing tendency with the increased wind speeds, because a higher wind speed will not only result in more transferred charges as discussed before, but also more importantly contribute a higher charge transfer rate. This set of results not only indicates a high power output of the R-TENG as driven by a stronger wind, but also shows the potential of the R-TENG as a self-powered wind speed sensor. Besides the magnitudes of the electrical outputs from the R-TENG, the information of the wind speed is also reflected by the time interval between two adjacent peaks, in other words, the number of peaks in a certain time. This is because the higher wind speed will drive a faster rotation of the rotor blade so that it will increase the frequency of the output. This relationship has been summarized in Figure S3, which shows a very good linear trend. Thus, by using a counter to calculate the number of peaks within a certain time, the corresponding wind speed can also be accurately obtained. Based on the above discussion, the R-TENG can be used as a self-powered active sensor for real-time wind speed detection.

Because of the viability to work at relatively low wind speed, this demonstrated R-TENG can be used to

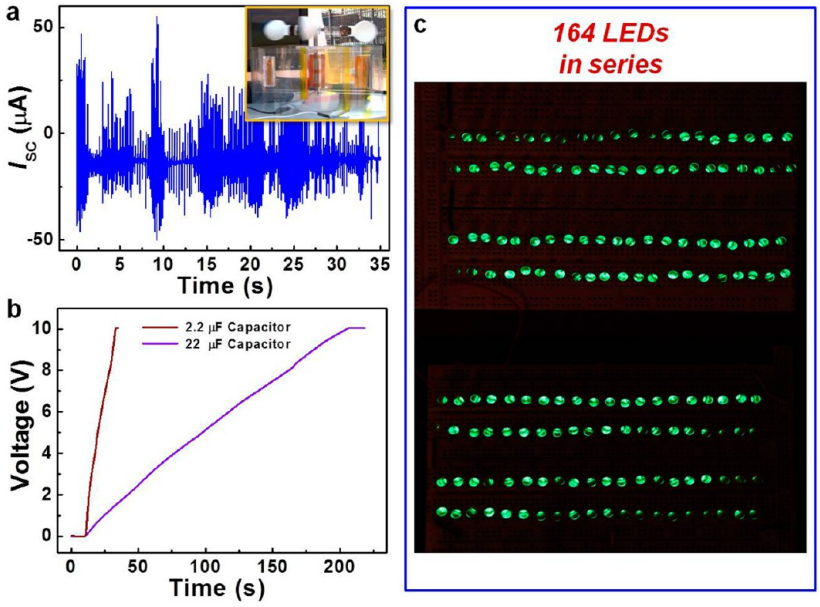

Figure 5. Applications of the R-TENG. (a) The R-TENG generating electricity from the wind blow in outdoor area; the inset is the picture of the R-TENG working under the wind blow in outdoor area. (b andc) The R-TENG used as a power source to (b) charge capacitors and (c) directly light up 164 commercial LEDs.

effectively harvest the energy from natural wind outside of an office building! As shown in Figure 5a and Video S1, when the modest wind blew through R-TENG, it generated electricity with a maximum I_{SC} of over 50 μA. It can be noticed that there was an obvious vibration in the current output, because of the fluctuation/turbulence in the wind speed at the outdoor area. As we have discussed, through analyzing this varied electrical output signal, the real-time wind speed at any given moment can be obtained. In many cases, the fluctuated electrical output generated from the natural wind needs to be stored for further use. Figure 5b shows the charging curves of two capacitors (2.2 and 22 μF, respectively) by the R-TENG at a wind scale of ~6 BF. These capacitors were charged by the R-TENG from empty to 10 V within a few seconds (27 s for 2.2 μF capacitor and 213 s for 22 μF capacitor, respectively), which indicates a high efficiency of converting the wind energy to the stored electrical energy. Furthermore, in some other cases, the instantaneous output of the R-TENG can be used to directly drive a number of electronic devices simultaneously. As shown in Figure 5c and Video S2, 164 serial-connected commercial LEDs were lit up by the wind-generated electricity from the R-TENG.

Compared to the conventional wind energy harvesting techniques, such as the electromagnetic-induction-based wind turbines, this new R-TENG has several unique advantages due to its novel design. First, since the R-TENG does not require any complex transmission units (such as gears and cranks), coils, or electromagnets, it is easy in fabrication, compact in volume, light in weight and a lot cheaper in cost. Thus, this design of the R-TENG is not only suitable for large-scale energy harvesting or civil power consumption, but also possible to be made into small and portable power sources for personal electronics. Importantly, R-TENG can be used for harvesting tiny scale wind or liquid flow energy around our houses, because it can be driven by a low speed wind! Furthermore, owing to a distinct relationship between the wind speed and the characteristics of the generated electrical outputs, the R-TENG can be used as a self-powered wind speed sensor.

CONCLUSION

In summary, we have demonstrated an innovative type of triboelectric nanogenerator based on the traditional vertical wind-cup structure for effectively harvesting wind energy, especially weak-wind available outdoors. By hybridizing the two basic modes for the first time, the R-TENG generated an open-circuit voltage of 250 V and a short-circuit current of 0.25 mA with a maximum power of 62.5 mW at the wind speed of 15 m/s, which is capable to either light up hundreds of commercial LEDs directly or efficiently charge energy storage units. Furthermore, based on the relationship between the electric output and the wind speed, the TENG can potentially be used as a self-powered wind speed sensor. It is the first time that triboelectric nanogenerators are combined with traditional wind power technology, which shows a number of advantages over the electromagnetic induction based technology. This invention may introduce a novel operation mechanism for wind generators and create a new development area of the wind power using

nanostructured surfaces of conventional materials. Furthermore, this technology can also be extended for harvesting energy from ocean current, so nanotechnology will soon reach our daily life.

METHODS

Fabrication of the Nanowire-like Structures on the Surface of PTFE Film. A 50-μm-thick PTFE film was first washed with menthol, isopropyl alcohol, and deionized water, consecutively, and then blown dry with nitrogen. Subsequently, a thin layer of Au nanoparticles, which can directly be used as "nanomasks" for the etching process, was deposited onto the PTFE surface using a DC sputter. Then, the inductively coupled plasma (ICP) reactive ion etching was used to produce the aligned nanowire-like structures on the surface. Specifically, Ar, O_2, and CF_4 gases were introduced in the ICP chamber with flow ratio of 15.0, 10.0, and 30.0 sccm, respectively. One power source of 400 W was used to generate a large density of plasma and the other power of 100 W was used to accelerate the plasma ions. The PTFE film was etched for 40 s, to get the nanowire-like structures with an average thickness of ~700 nm.

Conflict of Interest: The authors declare no competing financial interest.

Supporting Information Available: More detailed information about the electric output of the R-TENG upon one contacting and sliding, the effect of the different structures on the electric output of the devices, and the relationship between the wind speed and the number of I_{SC} peaks per second. This material is available free of charge *via* the Internet at http://pubs.acs.org.

Acknowledgment. Research was supported by U.S. Department of Energy, Office of Basic Energy Sciences under Award DEFG02- 07ER46394, NSF, and the Knowledge Innovation Program of the Chinese Academy of Sciences (Grant KJCX2-YW-M13). Yannan Xie thanks the support from the Chinese Scholars Council. Patents have been filed to protect the reported technologies.

REFERENCES AND NOTES

1. Wang, Z. L. Towards Self-Powered Nanosystems: From Nanogenerators to Nanopiezotronics. *Adv. Funct. Mater.* **2008**, *18*, 3553–3567.
2. Wang, Z. L.; Zhu, G.; Yang, Y.; Wang, S. H.; Pan, C. F. Progress in Nanogenerators for Portable Electronics. *Mater. Today* **2012**, *15*, 532–543.
3. Wang, Z. L.; Song, J. H. Piezoelectric Nanogenerators Based on Zinc Oxide Nanowire Arrays. *Science* **2006**, *312*, 242–246.
4. Wang, X. D.; Song, J. H.; Liu, J.; Wang, Z. L. Direct-Current Nanogenerator Driven by Ultrasonic Waves. *Science* **2007**, *316*, 102–105.
5. Qin, Y.; Wang, X. D.; Wang, Z. L. Microfibre-Nanowire Hybrid Structure for Energy Scavenging. *Nature* **2008**, *451*, 809–U5.
6. Yang, R. S.; Qin, Y.; Dai, L. M.; Wang, Z. L. Power Generation with Laterally Packaged Piezoelectric Fine Wires. *Nat. Nanotechnol.* **2009**, *4*, 34–39.
7. Xu, S.; Qin, Y.; Xu, C.; Wei, Y. G.; Yang, R. S.; Wang, Z. L. Self-Powered Nanowire Devices. *Nat. Nanotechnol.* **2010**, *5*, 366–373.
8. Tapia, A.; Tapia, G.; Ostolaza, J. X.; Saenz, J. R. Modeling and Control of a Wind Turbine Driven Doubly Fed Induction Generator. *IEEE Trans. Energy Convers.* **2003**, *18*, 194–204.
9. Herbert, G. M. J.; Iniyan, S.; Sreevalsan, E.; Rajapandian, S. A Review of Wind Energy Technologies. *Renew. Sust. Energ. Rev.* **2007**, *11*, 1117–1145.
10. Bressers, S.; Avirovik, D.; Vernieri, C.; Regan, J.; Chappell, S.; Hotze, M.; Luhman, S.; Lallart, M.; Inman, D.; Priya, S. Small-Scale Modular Windmill. *Am. Ceram. Soc. Bull.* **2010**, *89*, 34–40.
11. Ackermann, T.; Soder, L. Wind Energy Technology and Current Status: a Review. *Renewable Sustainable Energy Rev.* **2000**, *4*, 315–374.
12. Priya, S.; Chen, C. T.; Fye, D.; Zahnd, J. Piezoelectric Windmill: A Novel Solution to Remote Sensing. *Jpn. J. Appl. Phys.,Part 2* **2005**, *44*, L104–L107.
13. Priya, S. Modeling of Electric Energy Harvesting Using Piezoelectric Windmill. *Appl. Phys. Lett.* **2005**, *87*, 184101.
14. Myers, R.; Vickers, M.; Kim, H.; Priya, S. Small Scale Windmill. *Appl. Phys. Lett.* **2007**, *90*, 054106.
15. Fan, F. R.; Tian, Z. Q.; Wang, Z. L. Flexible Triboelectric Generator. *Nano Energy* **2012**, *1*, 328–334.
16. Fan, F. R.; Lin, L.; Zhu, G.; Wu, W. Z.; Zhang, R.; Wang, Z. L. Transparent Triboelectric Nanogenerators and Self-Powered Pressure Sensors Based on Micropatterned Plastic Films. *Nano Lett.* **2012**, *12*, 3109–3114.
17. Grzybowski, B. A.; Winkleman, A.; Wiles, J. A.; Brumer, Y.; Whitesides, G. M. Electrostatic Self-Assembly of Macroscopic Crystals Using Contact Electrification. *Nat. Mater.* **2003**, *2*, 241–245.
18. Kalsin, A. M.; Fialkowski, M.; Paszewski, M.; Smoukov, S. K.; Bishop, K. J. M.; Grzybowski, B. A. Electrostatic Self-Assembly of Binary Nanoparticle Crystals with a Diamond-like Lattice. *Science* **2006**, *312*, 420–424.
19. McCarty, L. S.; Whitesides, G. M. Electrostatic Charging Due to Separation of Ions at Interfaces: Contact Electrification of Ionic Electrets. *Angew. Chem., Int. Ed.* **2008**, *47*, 2188–2207.
20. Baytekin, H. T.; Patashinski, A. Z.; Branicki, M.; Baytekin, B.; Soh, S.; Grzybowski, B. A. The Mosaic of Surface Charge in Contact Electrification. *Science* **2011**, *333*, 308–312.
21. Zhu, G.; Pan, C. F.; Guo, W. X.; Chen, C. Y.; Zhou, Y. S.; Yu, R. M.; Wang, Z. L. Triboelectric-Generator-Driven Pulse Electrodeposition for Micropatterning. *Nano Lett.* **2012**, *12*, 4960–4965.
22. Wang, S. H.; Lin, L.; Wang, Z. L. Nanoscale Triboelectric-Effect-Enabled Energy Conversion for Sustainably Powering Portable Electronics. *Nano Lett.* **2012**, *12*, 6339–6346.
23. Zhu, G.; Lin, Z. H.; Jing, Q. S.; Bai, P.; Pan, C. F.; Yang, Y.; Zhou, Y. S.; Wang, Z. L. Toward Large-Scale Energy Harvesting by a Nanoparticle-Enhanced Triboelectric Nanogenerator. *Nano Lett.* **2013**, *13*, 847–853.
24. Wang, S. H.; Lin, L.; Xie, Y. N.; Jing, Q. S.; Niu, S. M.; Wang, Z. L. Sliding-Triboelectric Nanogenerators Based on In-Plane Charge-Separation Mechanism. *Nano Lett.* **2013**, *13*, 2226–2233.
25. Zhu, G.; Chen, J.; Liu, Y.; Bai, P.; Zhou, Y. S.; Jing, Q. S.; Pan, C. F.; Wang, Z. L. Linear-Grating Triboelectric Generator Based on Sliding Electrification. *Nano Lett.* **2013**, *13*, 2282–2289.
26. Lin, L.; Wang, S. H.; Xie, Y. N.; Jing, Q. S.; Niu, S. M.; Hu, Y. F.; Wang, Z. L. Segmentally Structured Disk Triboelectric Nanogenerator for Harvesting Rotational Mechanical Energy. *Nano Lett.* **2013**, *13*, 2916–2923.
27. Diaz, A. F.; Felix-Navarro, R. M. A Semi-Quantitative Tribo-Electric Series for Polymeric Materials: the Influence of Chemical Structure and Properties. *J. Electrost.* **2004**, *62*, 277–290.
28. Fang, H.; Wu, W. Z.; Song, J. H.; Wang, Z. L. Controlled Growth of Aligned Polymer Nanowires. *J. Phys. Chem. C* **2009**, *113*, 16571–16574.
29. Lee, L. H. Dual Mechanism for Metal-Polymer Contact Electrification. *J. Electrost.* **1994**, *32*, 1–29.
30. Watson, P. K.; Yu, Z. Z. The Contact Electrification of Polymers and the Depth of Charge Penetration. *J. Electrost.* **1997**, *40–1*, 67–72.
31. Saurenbach, F.; Wollmann, D.; Terris, B. D.; Diaz, A. F. Force Microscopy of Ion-Containing Polymer Surfaces—Morphology and Charge Structure. *Langmuir* **1992**, *8*, 1199–1203.